

Supporting Information

Distance Measurement of a Non-covalently Bound Y@C₈₂ Pair with Double Electron Electron Resonance Spectroscopy

Guzmán Gil-Ramírez,^{*,a,b,c} Anokhi Shah,^d Hassane El Mkami,^d Kyriakos Porfyraakis,^c G. Andrew D. Briggs,^c John J. L. Morton,^e Harry L. Anderson^b and Janet E. Lovett^d

^a School of Chemistry, University of Lincoln, Joseph Banks Laboratories, Lincoln, LN6 7DL, UK.

^b Chemistry Research Laboratory, Department of Chemistry, University of Oxford, 12 Mansfield Road, Oxford, OX1 3TA, UK.

^c Department of Materials, University of Oxford, Parks Road, Oxford, OX1 3PH, UK.

^d SUPA School of Physics and Astronomy, University of St Andrews, St Andrews, KY16 9SS, UK.

^e London Centre for Nanotechnology, UCL, 17-19 Gordon St, London WC1H 0AH, UK.

*Email: ggilramirez@lincoln.ac.uk

Table of Contents

Synthesis:

a. General procedures	S2
b. Synthesis of compounds	S3
c. Characterization data for compound 1	S6

Titration data:	S12
------------------------------	-----

Molecular Modelling:	S14
-----------------------------------	-----

EPR data:	S15
------------------------	-----

References:	S20
--------------------------	-----

Scheme S.1. Synthetic pathway for the synthesis of 5 and 1	S3
---	----

Table S.1. Q-band DEER experimental parameters.....	S16
--	-----

Figure S.1. HPLC-GPC traces of 1	S6
--	----

Figure S.2. MALDI-MS spectrum of 1	S7
--	----

Figure S.3. ¹ H NMR Spectrum of 1	S8
--	----

Figure S.4. ¹ H ¹ H NOESY Spectrum of 1	S9
---	----

Figure S.5. ¹ H DOSY Spectrum of 1	S10
---	-----

Figure S.6. ¹ H DOSY Spectrum of 3	S11
---	-----

Figure S.7. Titration data for Y@C ₈₂ and 1 in toluene.....	S12
--	-----

Figure S.8. Speciation diagram for (Y@C ₈₂) ₂ • 1	S13
--	-----

Figure S.9. Molecular modelling of (Y@C ₈₂) ₂ • 1	S14
--	-----

Figure S.10. Echo-detected field sweeps of (Y@C ₈₂) ₂ • 1	S15
--	-----

Figure S.11. Pulsed EPR spin-echo decay curves of (Y@C ₈₂) ₂ • 1	S15
---	-----

Figure S.12. Relaxation measurements of (Y@C ₈₂) ₂ • 1	S16
---	-----

Figure S.13. Background corrected Q-band DEER experiments of (Y@C ₈₂) ₂ • 1	S17
--	-----

Figure S.14. Fast Fourier Transforms of Q-band DEER of (Y@C ₈₂) ₂ • 1	S17
--	-----

Figure S.15. Justification for Tikhonov Regularisation Parameter choice.....	S18
---	-----

Figure S.16. Three-pulse ESEEM data of (Y@C ₈₂) ₂ • 1	S19
--	-----

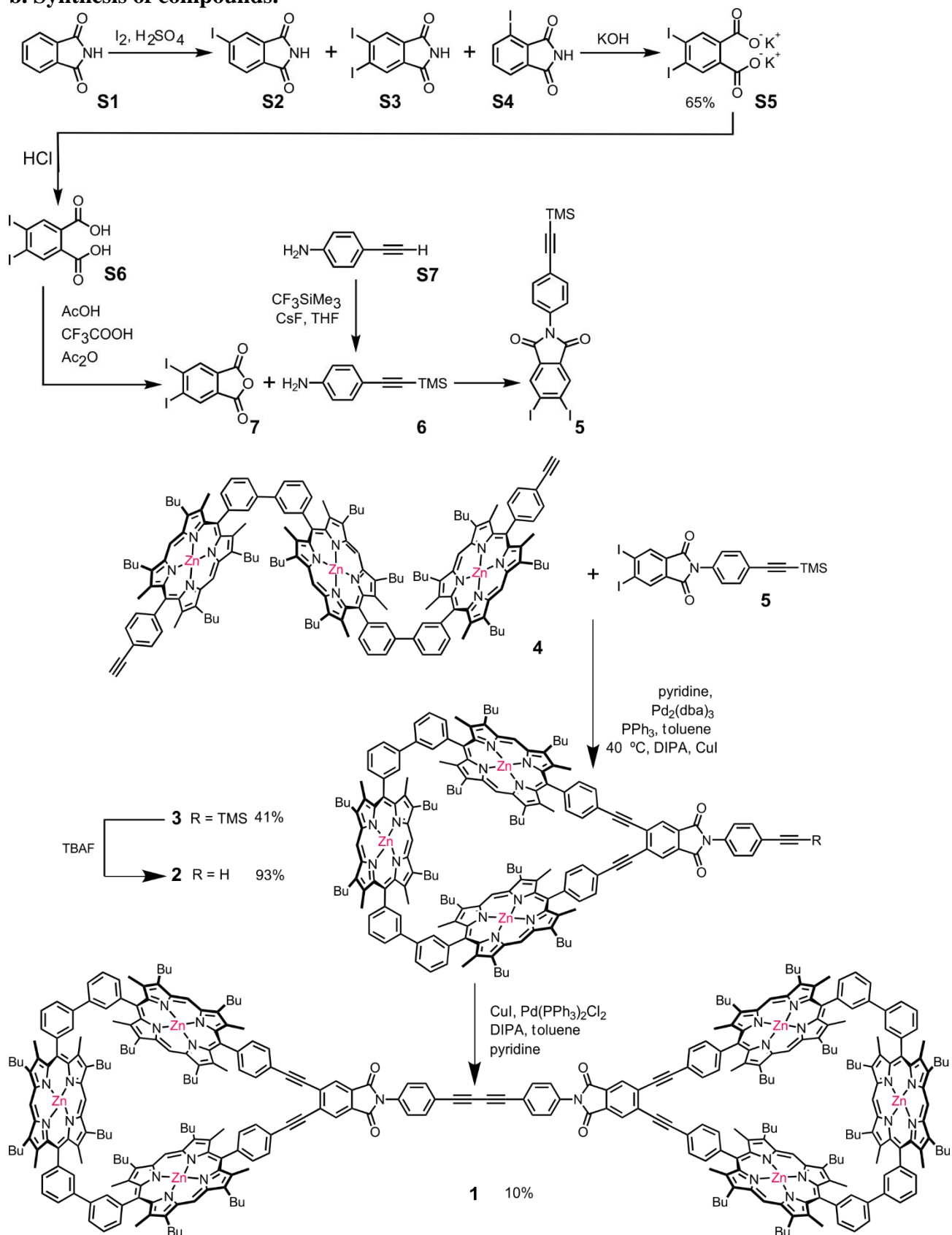
Figure S.17. Fourier Transformed ESEEM data for (Y@C ₈₂) ₂ • 1	S19
---	-----

Synthesis:

a. General procedures

The handling of all air/ water sensitive materials was carried out using Schlenk techniques. Freeze-thaw degassing was effected by freezing under nitrogen, pumping under vacuum, thawing in the absence of gases then re-freezing and pumping under vacuum. This process was repeated at least three times and the flask was saturated with nitrogen. Dried solvents were obtained by passing through alumina under nitrogen in a solvent purification system; Triethylamine was distilled from CaH_2 prior to use. Unless specified otherwise, all other solvents were used as commercially supplied. Where mixtures of solvents were used, ratios are reported by volume. Flash chromatography was carried out on silica gel 60 under positive pressure. Size exclusion chromatography (SEC) was carried out under gravity using cross-linked polystyrene Bio-Beads[®] SX-1 (200–400 mesh) in THF. HPLC-GPC was carried out in a VWR Hitachi HPLC instrument consisting of the following modules: DAD L2450; autosampler L-2200; quaternary pump L2130; column oven L2350. Analytical thin layer chromatography was carried out on aluminum backed silica gel 60 F254 plates. Visualization was achieved using UV light when necessary. All UV-Vis spectra were recorded in solution using a Perkin-Elmer Lambda 20 spectrometer (1 cm path length quartz cell). NMR spectra were recorded at room temperature, unless otherwise specified, using Bruker AV400 (400/100 MHz), Bruker AVII500 (500/125 MHz) and Bruker AVIII700 (700/175 MHz) instruments. ^1H and ^{13}C NMR spectra are reported in parts per million (ppm) relative to tetramethylsilane (δ_{H} 0.00); coupling constants (J) are given in Hertz and are quoted to the nearest 0.1 Hz. MALDI-TOF mass spectrometry was carried out using a Micromass MALDI micro MX spectrometer with DCTB matrix in positive mode detection. Only molecular ions and major peaks are reported. EPR measurements were taken using a Bruker Elexsys E580 using a 3 mm split ring resonator at X-band and high power (150 W) Q-band with an ER 5106QT-2w cylindrical resonator.

b. Synthesis of compounds.



Scheme S.1. Pathway for the synthesis of the phthalimide **5**, and cyclic trimer **1**.

Compound **S2** was synthesized by slightly modifications of procedure described by Terekhov *et al.*¹ We describe a different procedure for the purification and isolation, based on the results presented by Higgins *et al.*² Compound **6** was obtained following the procedure described by Ishizaki *et al.*³ Y@C₈₂ was obtained via the arc-discharge method, using yttrium-doped graphite rods (Toyo Tanso, Japan). The sample was isolated via recycling HPLC using pure toluene as eluent according to previously published methodology.⁴

4,5-Diiodophthalimide (S2):

To 20% fuming sulfuric acid (60 mL) was added phthalimide (14.5 g, 0.099 mmol) and iodine (25.4 g, 0.1 mmol). The reaction mixture was stirred vigorously and heated to 75-80°C during 24 hours. Then the mixture was poured into ice (400 g), and the precipitated solids were filtered off, washed twice with water, once with a 2% solution of K₂CO₃, once with a saturated solution of Na₂S₂O₃ and water again. Then the solid was dried in air, and the precipitate (15 g) was extracted with acetone (500 mL) in a soxhlet extractor for 48 hours. Almost all the solid in the filter cone was dissolved and extracted into an orange-red solution that was cooled to room temperature. Water (200 mL) was added to the acetone solution and concentrated to 300 mL total volume. A white solid precipitated and was collected by suction and dried (6.5 g). The ¹H-NMR in CDCl₃ showed a mixture of 4,5-diiodo (**S2**), 3,5-diiodo (**S3**) and 4-monoiodo (**S4**) phthalimides. Yield 6.5 g (15%) for the mixture of isomers. All the spectroscopic data of this compound are in agreement with those reported in the literature.¹

Potassium 4,5-diiodophthalate (S5) and monoanion (S6):

The mixture (1.65 g) obtained on the previous step (4,5- and 3,4-diiodophthalimides **S2**, **S3** and 4-monoiodo phthalimide **S4**) was dispersed in 10% aqueous KOH (40 mL) The mixture was refluxed in an oil bath at 115°C during 12 hours and then cooled to room temperature. The pH was carefully adjusted to pH = 5 using a 6M HCl solution. At that pH a white solid precipitates that corresponds mainly to product **S6**. The solid was collected by suction and dried over high vacuum to obtain compound **S6** (1.15 g) in a 65% yield. This white solid is very insoluble in any organic solvent. ¹H NMR (400 MHz; DMSO-*d*₆) δ 8.59 (s, 2H), 20.69 (bs, 1H). ¹³C NMR (125 MHz; DMSO-*d*₆) δ 112.9, 135.9, 143.8, 166.8.

4,5-Diiodophthalic anhydride (7):

Compound **7** was obtained from compound **S6**. Compound **S6** (50 mg) was dissolved in a mixture of acetic acid (5 mL), TFA (1 mL) and acetic anhydride (5 mL). The reaction mixture was stirred and heated at 120°C for 2 hours, then cooled to room temperature and solvent removed under vacuum to obtain an off-white solid (50 mg) in a quantitative yield. ¹H NMR (400 MHz; DMSO-*d*₆) δ 8.15 (s, 2H). ¹³C NMR (125 MHz; DMSO-*d*₆) δ 113.0, 134.3, 139.6, 167.5.

4,5-Diiodo N-(4-trimethylsilyl-ethynylphenyl)phthalimide (5):

In a flask containing 4,5-diiodo phthalic anhydride **7** (190 mg, 0.48 mmol) and 4-(TMS-ethynyl)aniline **6** (90 mg, 0.48 mmol) was added toluene (75 mL) and triethylamine (5 μL) and the flask was connected to a Dean-Stark apparatus. The mixture was stirred and refluxed (150°C) in an oil bath. After 24 hours the mixture was evaporated to dryness. The crude solid (290 mg) was purified by column chromatography (SiO₂) using dichloromethane as solvent. The first eluting compound corresponds to product **5**. Yield 97 mg (36%).

¹H NMR (400 MHz; CDCl₃) δ 0.27 (s, 9H), 7.39 (d, *J* = 8.4 Hz 2H), 7.58 (d, *J* = 8.4 Hz 2H), 8.42 (s, 2H); ¹³C NMR (125 MHz; CDCl₃) δ 0.1, 95.8, 104.2, 116.1, 123.4, 126.0, 131.2, 131.7, 132.8, 134.3, 165.3.

TMS-acetylene protected trimer of porphyrins (3):

Compound **3** was synthesized using a similar procedure as previously described.⁵

In a screw-capped Schlenk tube were introduced the terminal acetylene porphyrin trimer **4** (75.0 mg, 30.0 μmol), 4,5-diiodo-phthalimide **5** (17 mg, 30.0 μmol), $\text{Pd}_2(\text{dba})_3$ (8 mg, 9.0 μmol), triphenylphosphine (8 mg, 30.0 μmol) and CuI (1 mg, 8.0 μmol) and a magnetic stirrer bar. The tube was degassed by three high vacuum/argon cycles and then toluene (16.5 mL), of triethylamine (2.10 mL) and pyridine (0.85 mL) were introduced. The reaction was degassed by three cycles of freeze-pump-thaw and then warmed to room temperature. The reaction was then heated to 40 °C for 16 hours and then quenched by passing through a small silica plug with dichloromethane / 1% pyridine, and solvent was evaporated. The crude reaction mixture was purified by SEC (THF) with the major products eluting first corresponding to porphyrin polymers and the final eluting fraction was found to be the desired closed trimer **3**. Recrystallization from dichloromethane / MeOH gave a purple solid. Yield 35 mg (41%). ^1H NMR (500 MHz; CDCl_3 + 5% pyridine- d_5) δ 0.30 (s, 12H), 0.72 (t, J = 7.5 Hz, 12H), 0.84 (t, J = 7.5 Hz, 12H), 0.87 (t, J = 7.5 Hz, 12H), 1.38-1.53 (m, 24H), 1.87 (m, 24H), 2.41 (m, 12H), 2.42 (s, 24H), 3.70 (bs, 24H), 7.53 (d, J = 8.4 Hz, 2H), 7.65 (d, J = 8.4 Hz, 2H), 7.87 (t, J = 7.6 Hz, 4H), 7.88 (t, J = 7.6 Hz, 4H), 7.95 (d, J = 8.3 Hz, 2H), 8.00 (d, J = 7.5 Hz, 4H), 8.06 (d, J = 7.5 Hz, 2H), 8.13 (m, 4H), 8.26 (s, 4H), 8.31 (s, 2H), 8.38 (d, J = 8.4 Hz, 4H), 9.75 (s, 4H), 9.77 (s, 2H); ^{13}C NMR (125 MHz; CDCl_3 + 5% pyridine- d_5) δ 0.1, 13.9, 14.0, 15.4, 15.4, 15.5, 22.9, 23.1, 26.2, 29.7, 35.3, 88.2, 95.5, 96.9, 97.0, 99.5, 117.0, 118.3, 118.6, 121.5, 126.2, 126.5, 127.7, 127.8, 130.3, 130.7, 131.0, 131.5, 131.6, 131.7, 132.3, 132.4, 132.6, 133.6, 133.8, 136.5, 137.0, 137.2, 139.4, 142.7, 142.8, 143.0, 144.9, 145.1, 146.0, 146.1, 146.5, 146.7, 147.2, 147.3, 166.0; MS (MALDI, Dithranol) m/z calculated for $[\text{M}]^+$ 2778.27, found 2778.82.

Acetylene capped trimer of porphyrins (2): TMS protected porphyrin trimer **3** (25.0 mg, 9.0 μmol), was dissolved in dry THF (6 mL) and stirred at room temperature under nitrogen. To this solution was added a 1.0 M solution of TBAF in THF (45 μL , 45.0 μmol). The reaction was stirred for 30 minutes and then quenched by passing the crude reaction over a silica plug with THF. The pure product **3** (20 mg, red solid) was then used immediately in subsequent dimerization reaction. Yield 20 mg (93%) MS (MALDI, Dithranol) m/z calculated for $[\text{M}]^+$ 2707.24, found 2707.60.

Dimeric trimer of porphyrins (1)

In a screw-capped Schlenk tube were introduced with the terminal acetylene porphyrin trimer **2** (20.0 mg, 7.4 μmol), benzoquinone (1 mg, 9.2 μmol), $\text{Pd}(\text{PPh}_3)\text{Cl}_2$ (2 mg, 2.2 μmol), and CuI (0.4 mg, 2.2 μmol). The tube was degassed by three high vacuum/argon cycles and then toluene (1.0 mL), diisopropylamine (0.5 mL) and pyridine (1 μL) were introduced. The reaction was degassed by three cycles of freeze-pump-thaw and then warmed to room temperature. The reaction was then stirred for 16 hours and then quenched by passing through a small silica plug with dichloromethane / 1% pyridine, and solvent was evaporated. The crude reaction mixture was purified by SEC (THF) with the major products eluting first corresponding to porphyrin polymers and the final eluting fraction was found to be the desired dimer **1**. Recrystallization from dichloromethane / MeOH gave a purple solid. Yield 2 mg (10%). ^1H NMR (500 MHz; CDCl_3 + 5% pyridine- d_5) δ 0.72 (t, J = 7.5 Hz, 12H), 0.84 (t, J = 7.5 Hz, 12H), 0.87 (t, J = 7.5 Hz, 12H), 1.38-1.53 (m, 24H), 1.87 (m, 24H), 2.41 (m, 12H), 2.42 (s, 24H), 3.70 (bs, 24H), 7.53 (d, J = 8.4 Hz, 2H), 7.65 (d, J = 8.4 Hz, 2H), 7.87 (t, J = 7.6 Hz, 4H), 7.88 (t, J = 7.6 Hz, 4H), 7.95 (d, J = 8.3 Hz, 2H), 8.00 (d, J = 7.5 Hz, 4H), 8.06 (d, J = 7.5 Hz, 2H), 8.13 (m, 4H), 8.26 (s, 4H), 8.31 (s, 2H), 8.38 (d, J = 8.4 Hz, 4H), 9.75 (s, 4H), 9.77 (s, 2H); MS (MALDI, Dithranol) m/z calculated for $[\text{M}]^+$ 5411.5, found 5411.5. λ_{max} (Toluene) / nm (log ϵ): 423 (6.37), 552 (5.25), 585 (4.90).

c. Characterization data for compound 1:

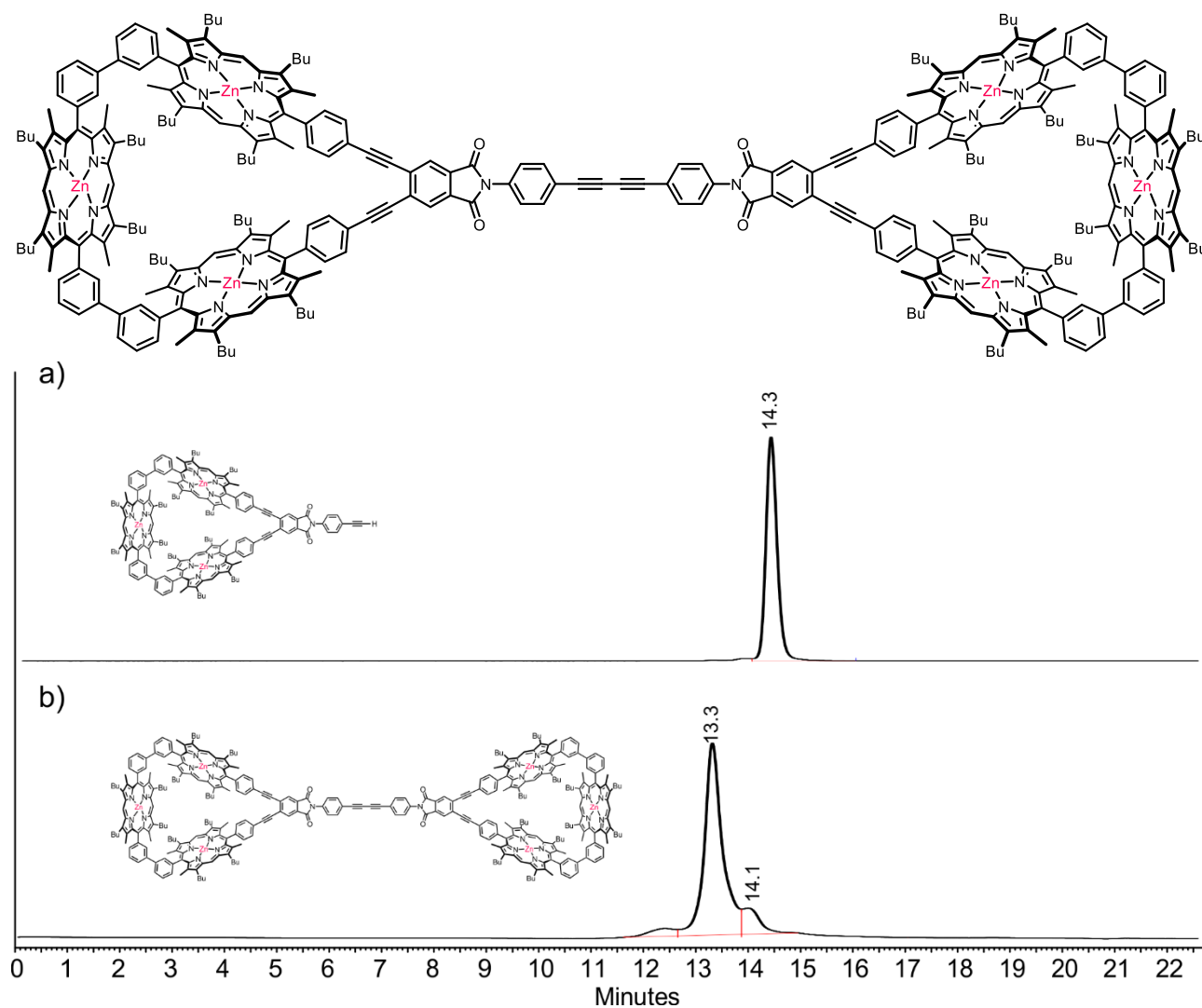


Figure S.1 – HPLC-GPC traces of: a) acetylene capped cyclic trimer **2**; b) fraction eluted on gravity SEC column corresponding to product **1**. GPC conditions: Polymer labs PLgel 3 μm 300x7.5 mm MIXED-E column (two columns in tandem); 1 mL/min; Toluene with 10% pyridine as eluent; UV detector at 420 nm; sample 1 mg/mL; 20 μL injected.

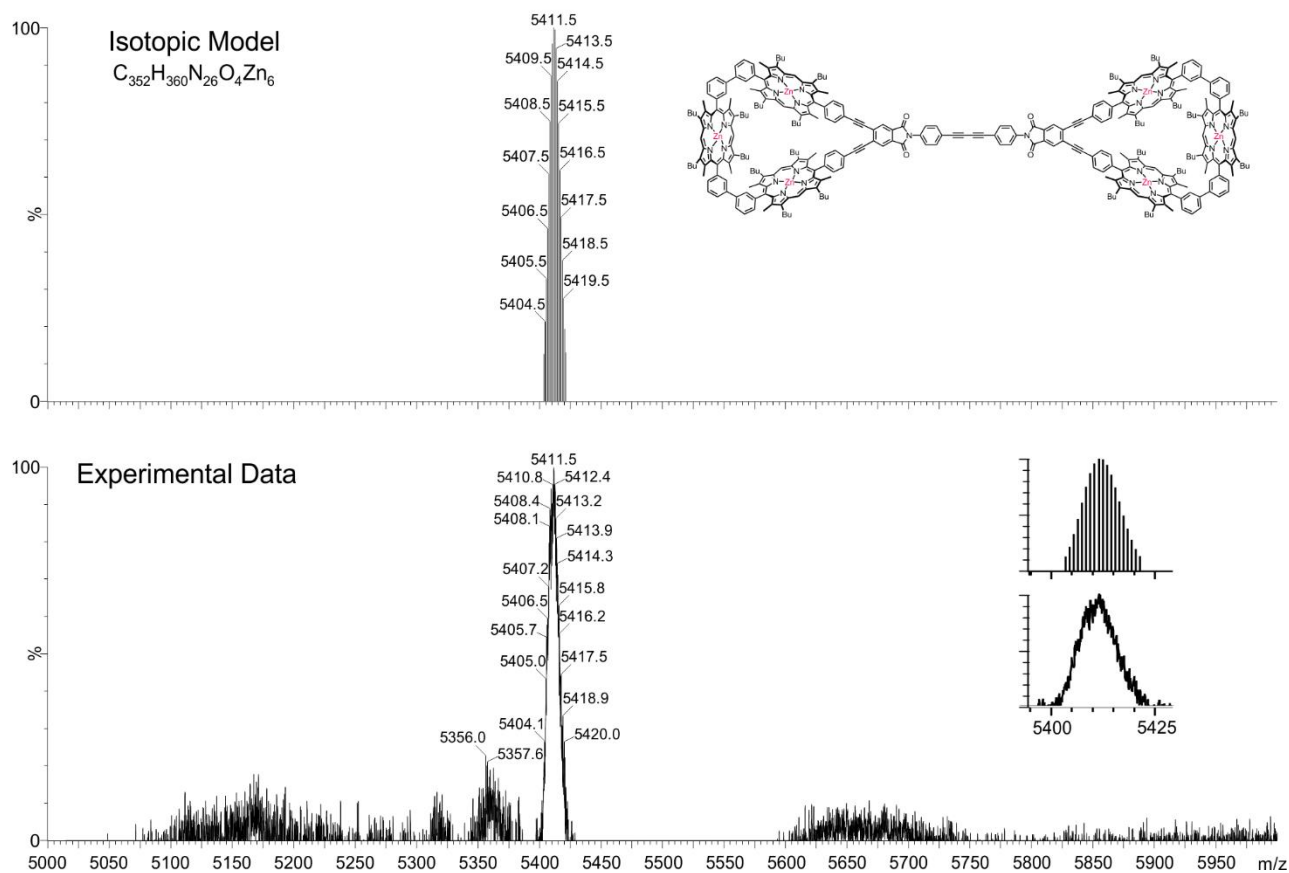


Figure S.2 – MALDI-MS spectrum of **1**. Upper trace: Calculated spectrum; bottom trace: observed spectrum. Inset shows a zoom of the isotopic pattern.

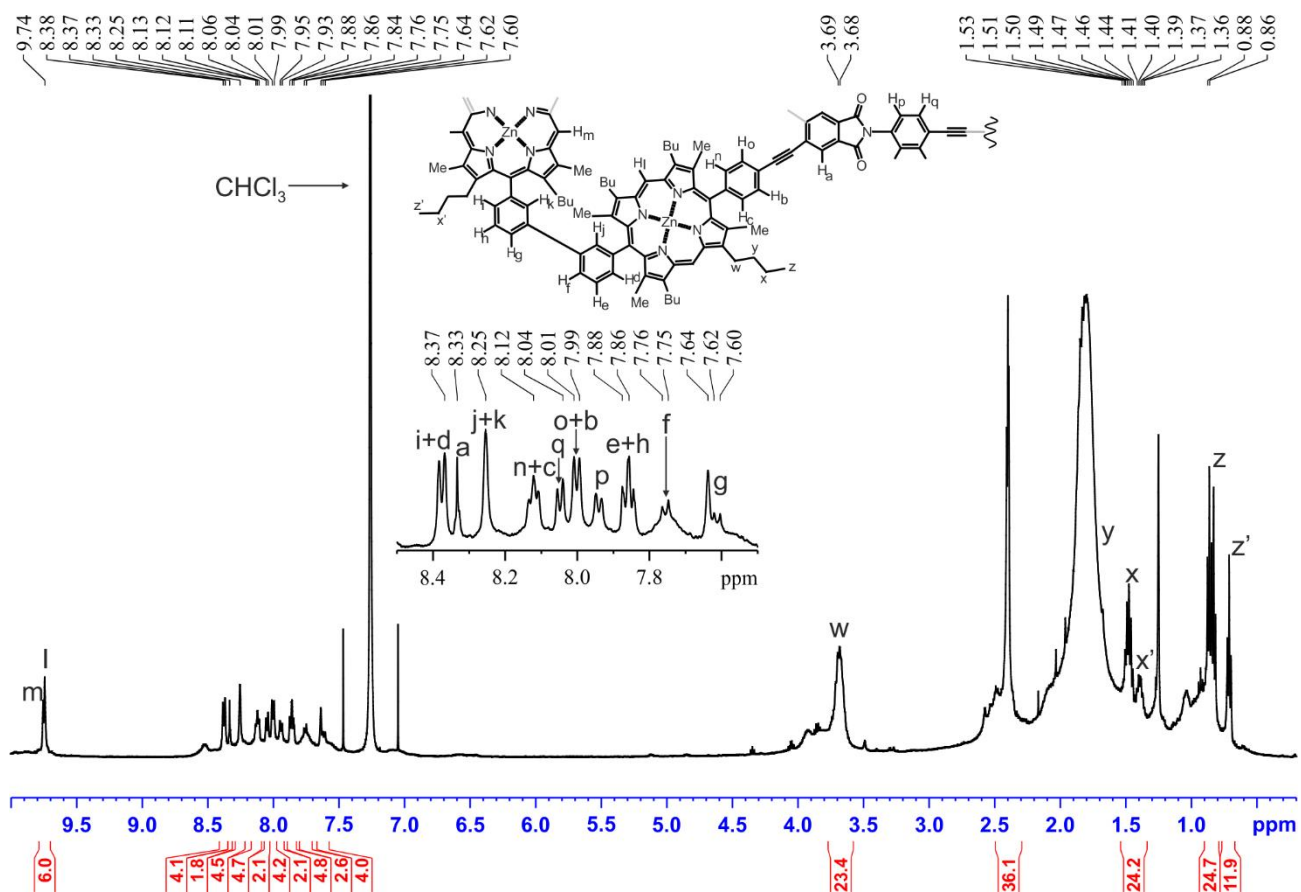


Figure S.3 – ¹H NMR spectrum of **1** (500 MHz, CDCl₃/5% pyridine-*d*₅, 298 K). Primed letters indicate inequivalent protons.

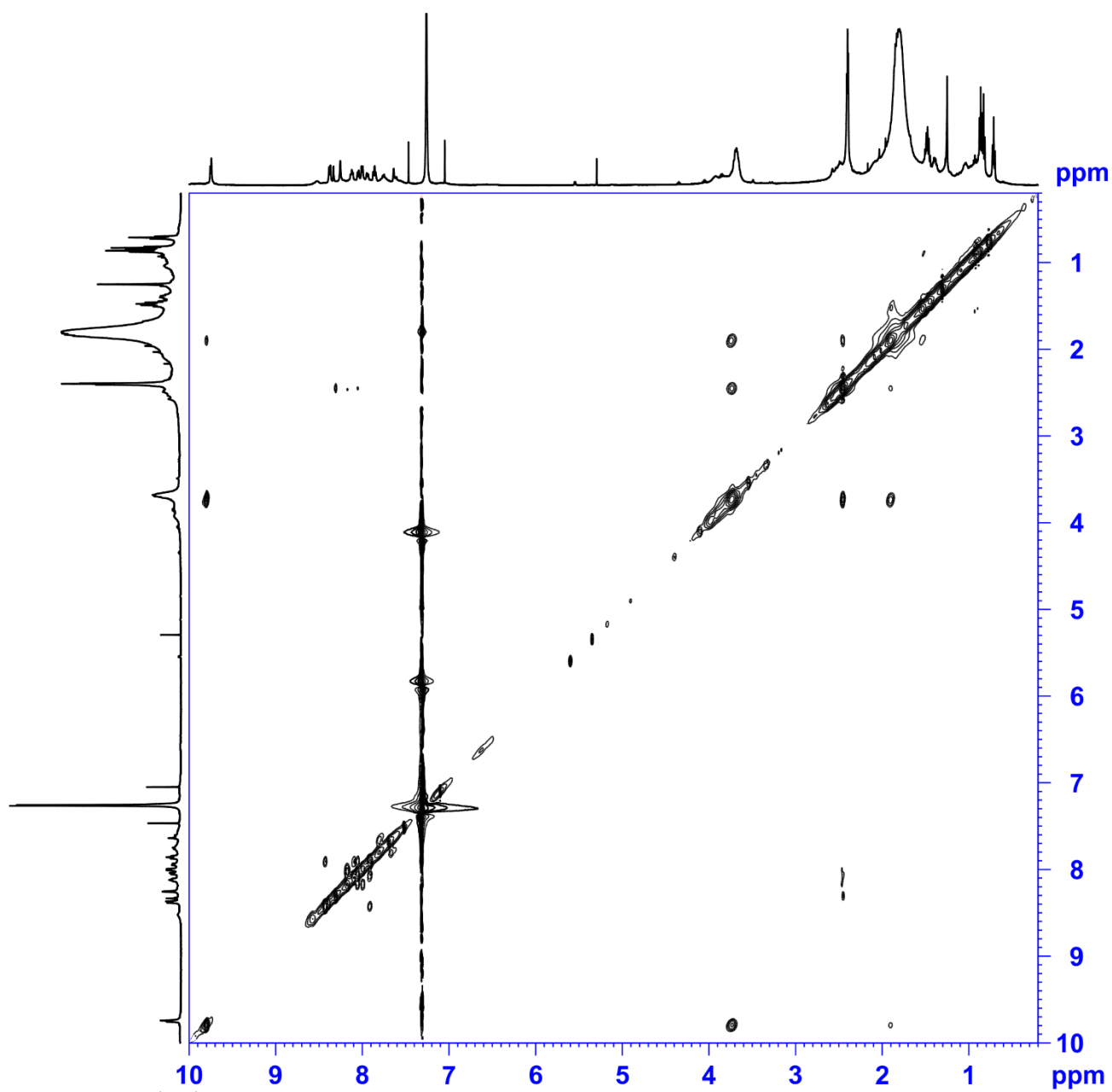


Figure S.4 – ^1H ^1H NOESY spectrum for **1** (500 MHz, $\text{CDCl}_3/5\%$ pyridine- d_5 , 298 K).

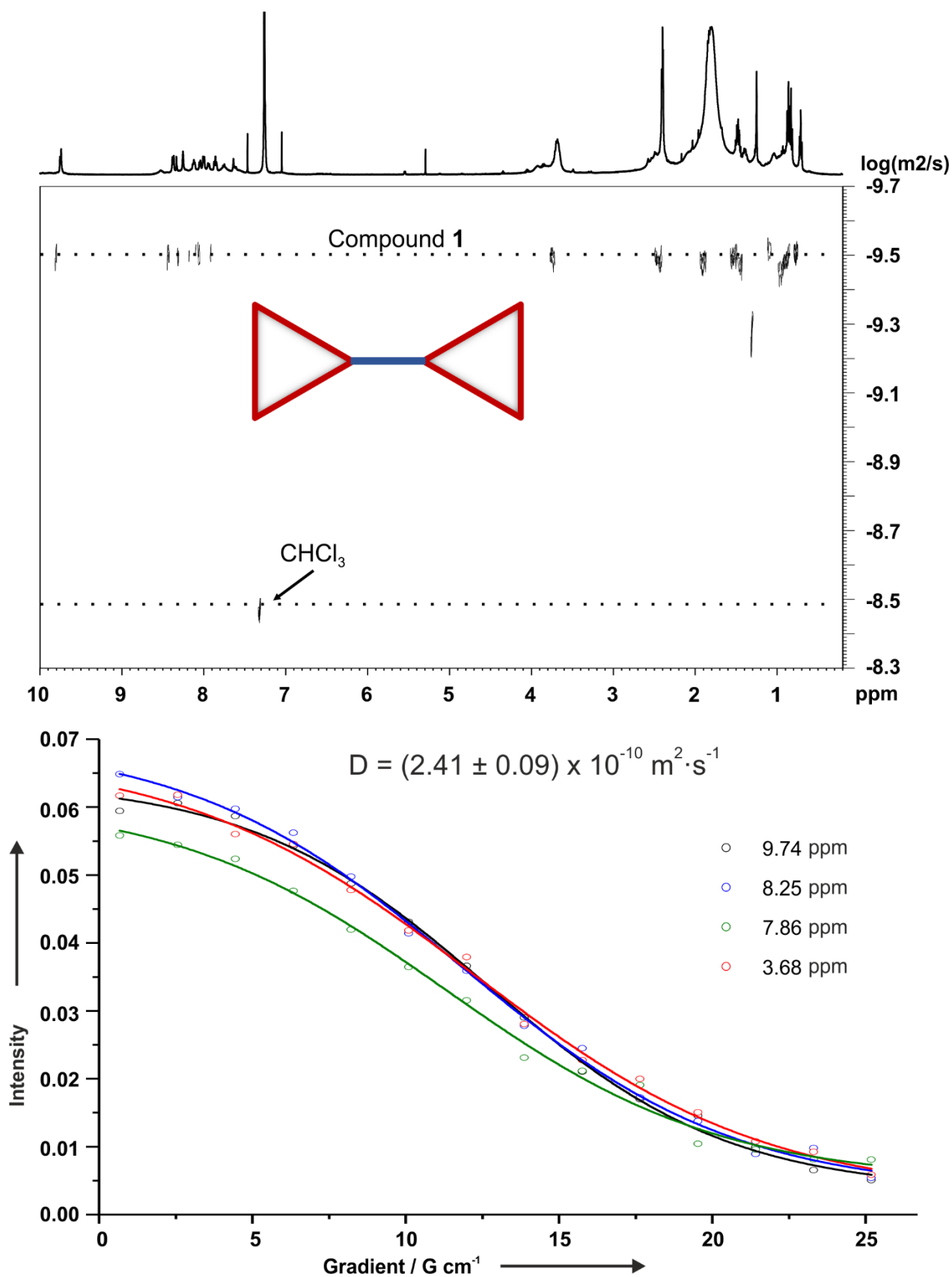


Figure S.5 – ^1H DOSY spectrum of **1** (500 MHz, $\text{CDCl}_3/5\%$ pyridine- d_5 , 298 K).

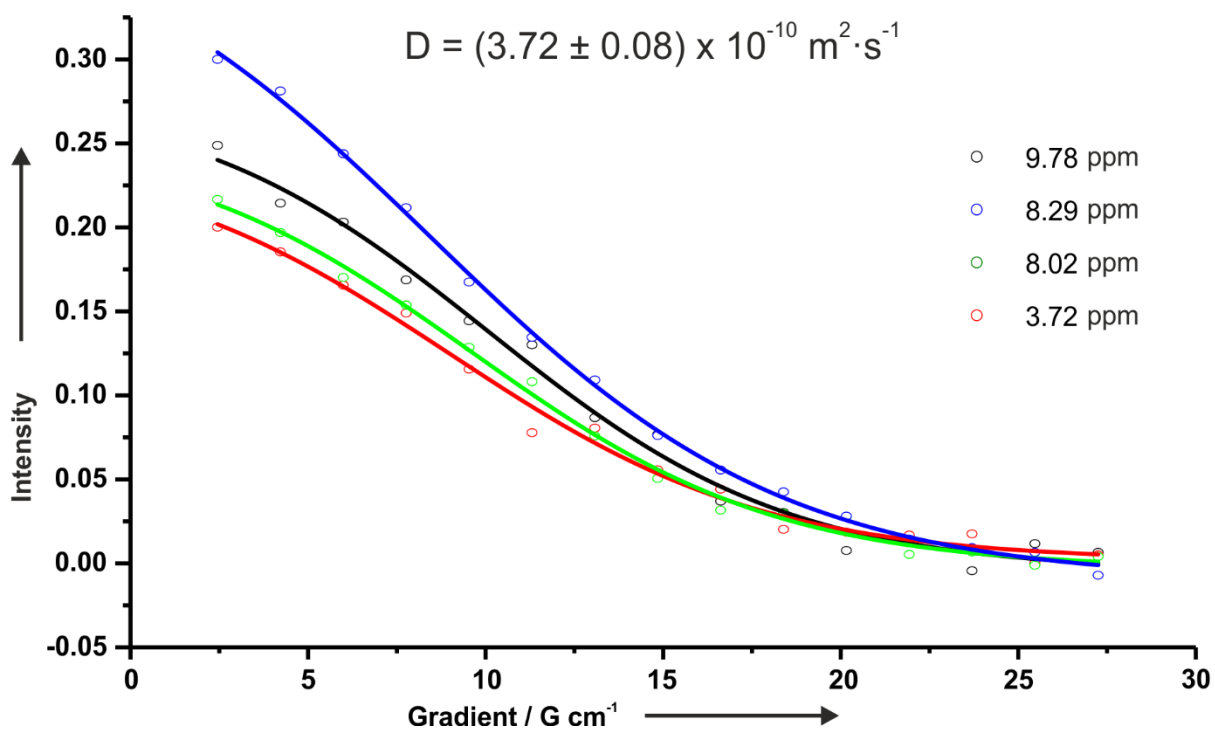
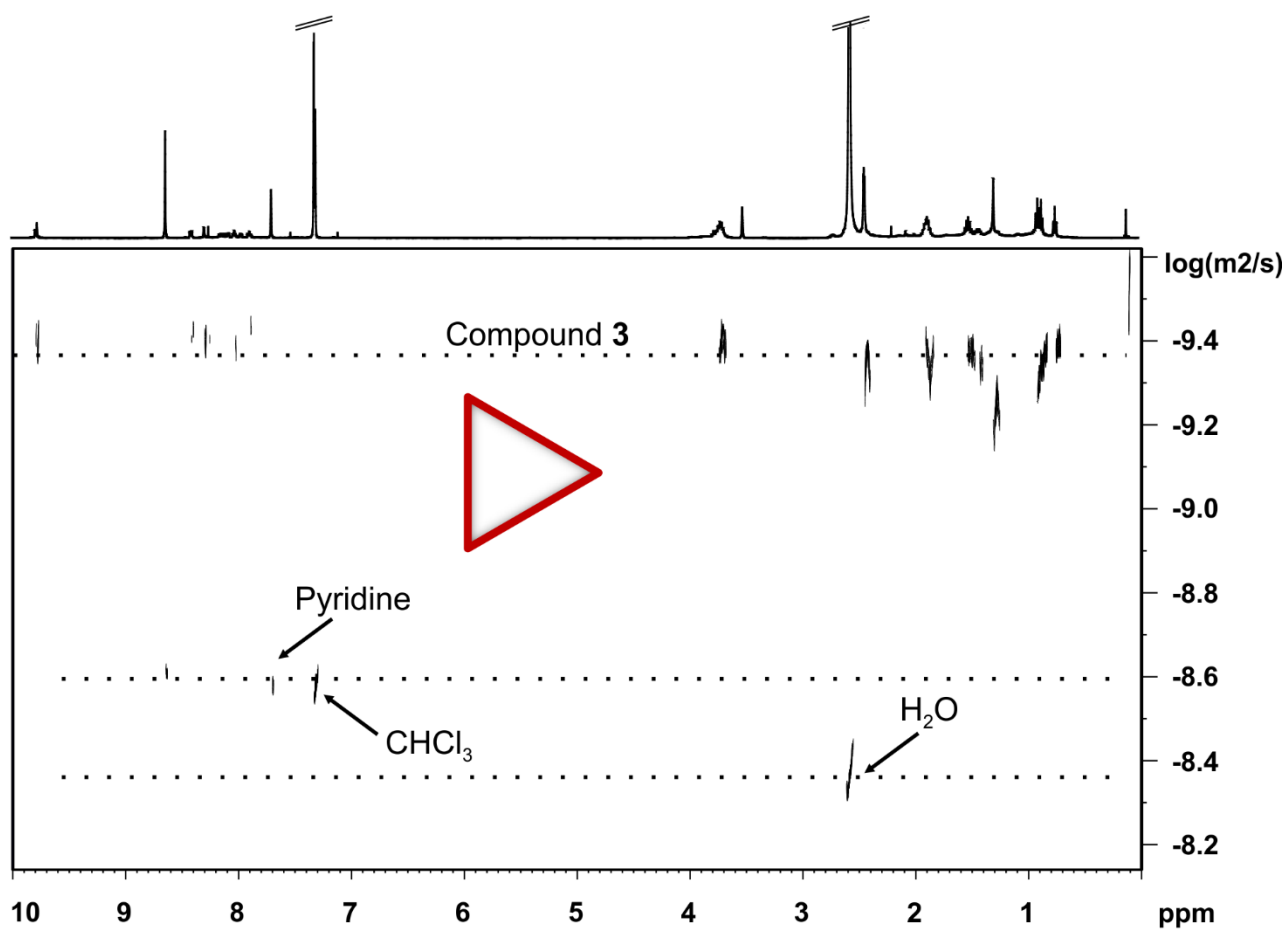


Figure S.6 – ¹H DOSY spectrum of **3** (500 MHz, CDCl₃/1% pyridine, 298 K).

The DOSY plot of **1** shows that all proton corresponding to the compound diffuse at the same rate proving the integrity of the compound. As expected, compound **1** (Figure S.5) diffuses less rapidly than compound **3** (Figure S.6), implying that the hydrodynamic radius of the compound is larger than compound **3**.

Titration data for compound **1**:

The binding behavior of the dimer **1** to Y@C₈₂ was studied by UV-visible titration. The data (Figure S.7) was analyzed by non-linear curve fitting with the software Origin, assuming a 1:1 binding situation. The binding sites in the dimer molecules behave independently in their binding to Y@C₈₂ and therefore it was assumed that the system can be fitted to a 1:1 stoichiometry using concentration of binding site ([BS]=2×[H]) instead of concentration of host **1**. If this assumption were fulfilled in the actual system, isosbestic behavior would be expected. The actual titration shows minor deviation from isosbestic behavior, which may be due to slight initial aggregation. Nevertheless, using the described 1:1 model a fit (Figure S.7) is obtained but the curve is too sharp to give an accurate value for the binding constant. This behavior is similar to the previously reported one observed for compound **A** (Figure S.8) and the endohedral fullerene La@C₈₂ system.⁵

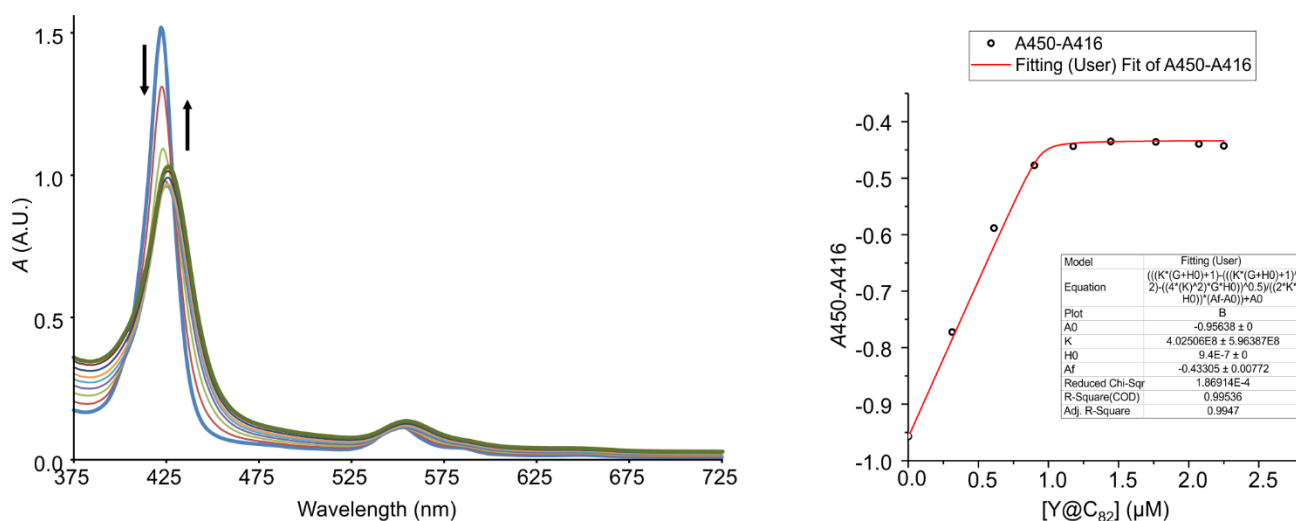
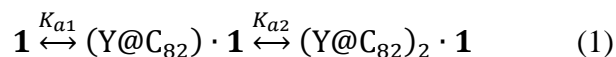


Figure S.7. UV-Visible titration of **1** with Y@C₈₂ in toluene at 25°C. The concentration of **1** was 0.47×10^{-6} mol/L. The system was fitted to a 1:1 stoichiometry using concentration of binding site instead of concentration of host ([BS] = 0.94×10^{-6} mol/L).

Receptor **A** displayed affinities ($K > 10^9$ M⁻¹) for C₈₆ and La@C₈₂ in toluene that were too large to be measured accurately by fluorescence titration technique.⁵ The binding sites in receptor **1** closely resemble the structure of the porphyrin trimer **A** (Figure S.8) therefore on the modelled system it was assumed that each binding site on **1** had a similar affinity for Y@C₈₂ ($K \sim 10^9$ M⁻¹) as **A**. The formation of a doubly-filled receptor **1** within a system with two identical independent binding sites can be described by equation 1:



We assume the binding of the fullerenes to the individual binding sites occurs independently, irrespectively of the binding sites being connected to each other. To model the population of the different species present in solution, the program HySS 2009 was used for providing speciation diagrams to present the distributions of the various complex species (**1**, $(Y@C_{82})\cdot\mathbf{1}$, $(Y@C_{82})_2\cdot\mathbf{1}$) that were formed at the selected concentration ranges.⁶ From the simulations (Figure S.8) we find that $[\mathbf{1}] = 10^{-6}$ M offers a good compromise between keeping the concentration low, to minimise spin-spin relaxation effects, while still affording 96% of the double bound species $(Y@C_{82})_2\cdot\mathbf{1}$ when just two equivalents of $Y@C_{82}$ are present.

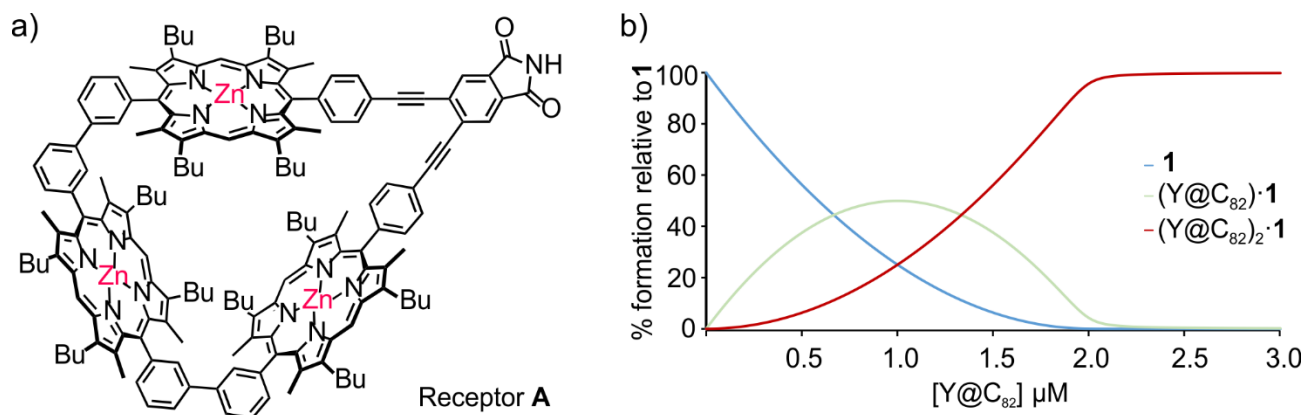


Figure S.8. a) Structure for receptor **A**.⁵ b) Simulated speciation diagram for $(Y@C_{82})_2\cdot\mathbf{1}$ complex formation at $[\mathbf{1}] = 1 \mu\text{M}$ and $K_{a1} = 4$ $K_{a2} = 2 \cdot 10^9 \text{ M}^{-1}$.

Molecular modelling:

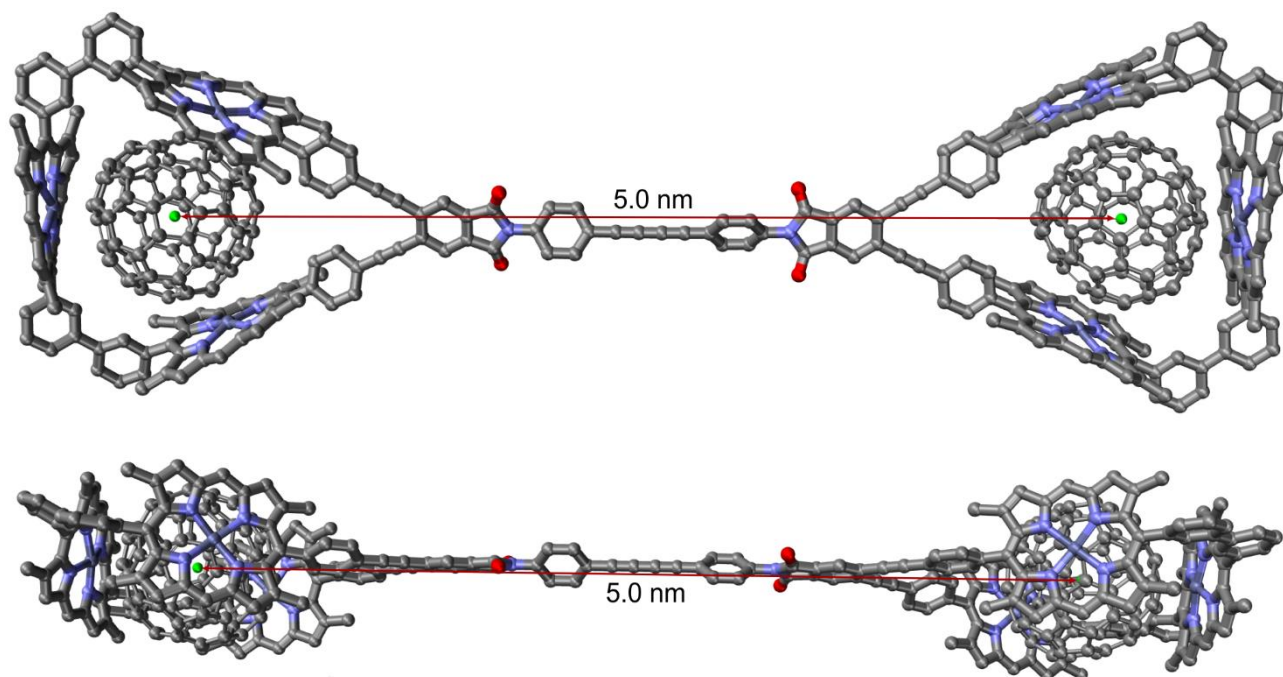


Figure S.9. Molecular models of $(Y@C_{82})_2 \cdot \mathbf{1}$ in balls and sticks representation. Endohedral Yttrium atoms have been omitted for clarity. The green ball inside the fullerene represents the centroid of the fullerene. a) top-view b) side-view. Structures minimized using the MM+ force field integrated in the HyperChemTM 8 package. Minimizations were performed using the steepest descent and Polak-Ribiere algorithms. The models demonstrate the elongated shape of **1** and the distance between the centroids of the two bound endohedral fullerenes.

EPR data:

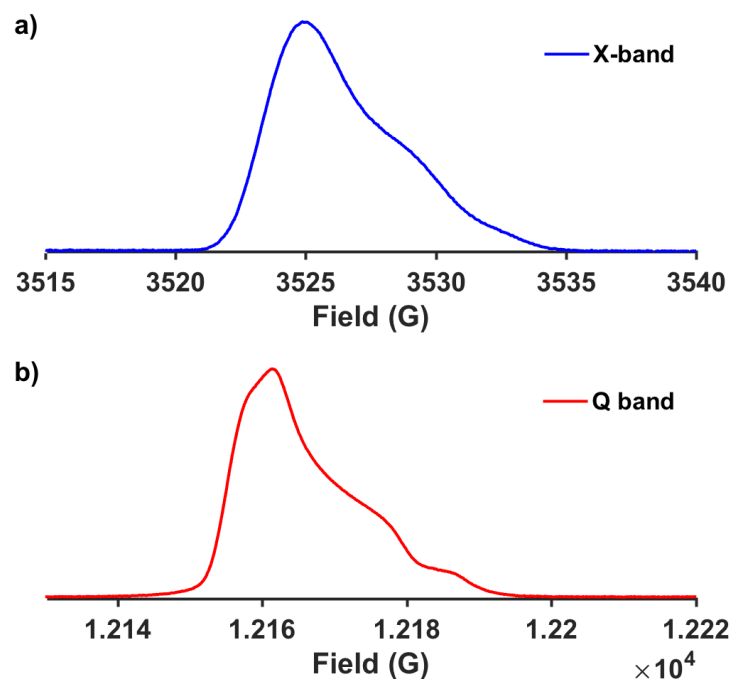


Figure S.10. Pulsed EPR echo-detected field-sweeps at 30 K for $(Y@C_{82})_2\bullet 1$ in deuterated toluene at a) X-band (9.87 GHz) and b) Q-band (34 GHz). The results indicate two major constituent isomers of $(Y@C_{82})$ with axial g-tensors.

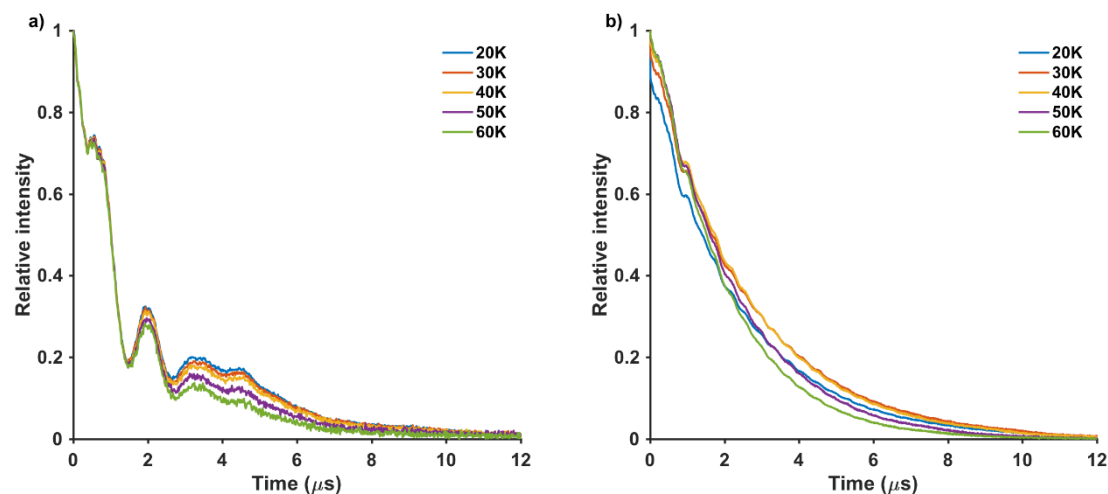


Figure S.11. Pulsed EPR spin-echo decay results for $(Y@C_{82})_2\bullet 1$ in deuterated toluene normalised to the maximum, measured at 10 K intervals between 20-60 K at a) X-band (9.87 GHz) and b) Q-band (34 GHz) at the magnetic field position corresponding to the maximum of the echo-detected field-swept spectra shown in Figure S.10. These data demonstrate only a gradual increase in decay rate with increasing temperature and show strong electron-nuclear hyperfine interactions at X-band.

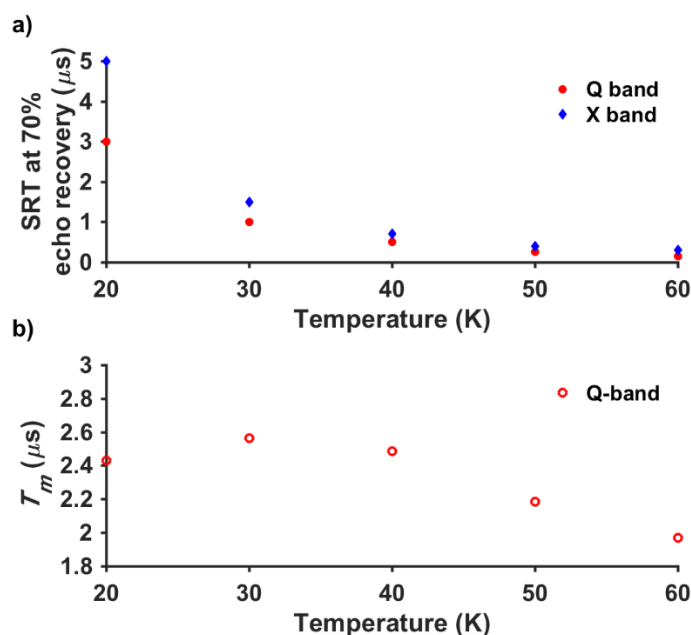


Figure S.12. Relaxation measurements of $(Y@C_{82})_2\bullet 1$ in deuterated toluene, measured at 10 K intervals between 20-60 K at both X (blue) and Q-band (red). a) T_1 measured through observing effect of the shot repetition time (SRT) of the echo. The values plotted are of the SRT at 70% echo intensity. b) T_m found using a single exponential fit (using Bruker's XEPR software) of the spin-echo decay results shown in Figure S.11. The large modulation depth of the electron spin echo envelope modulation (ESEEM) at X-band leads to problems reliably quantifying T_m . However, the T_m values are approximately the same at X and Q-bands.

Name	Field position for pump / G	Pump length / ns	Offset between pump and observer frequencies / MHz
DEER 1 (also shown in main paper)	12158 (low field shoulder of field-sweep)	22	56
DEER 2	12161 (maximum of signal)	22	56
DEER 3	12167	22	56
DEER 4	12158	22	81
DEER 5	12158	32	50

Table S.1. Q-band DEER experimental parameters for the time traces given in Figure S.13 and their respective Fourier Transforms in Figure S.14 used for measurements of $(Y@C_{82})_2\bullet 1$ in deuterated toluene. Observer pulse lengths were set at 32 ns with position at lower frequency than the pump pulse. The field values are shown in Figure S.10b.

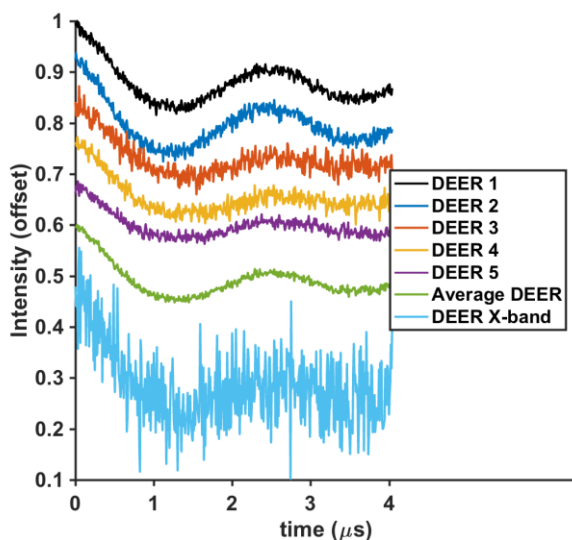


Figure S.13. Background corrected Q-band DEER experiments (using DeerAnalysis2016⁷), defined in Table S.1, compared to X-band DEER. The X-band DEER used a 40 ns pump pulse at 3525 G (see Figure S.10a) and 80 ns observer pulses 22 MHz lower frequency (~ 7.9 G higher field). These data show that the dipolar coupling is measured at both X and Q-band EPR frequencies; that the Q-band measurements have significantly improved signal-to-noise ratio due to the higher sensitivity achieved by the improved hardware performances at this frequency⁸ and reduced amplitude ESEEM at the higher frequency which effectively decreases the size of the available echo at X-band in the DEER experiment; and that, under the conditions used, major orientation selection was not observed by DEER since the frequency of the dipolar modulations remained the same. This is further demonstrated with the *Average DEER* shown in green which is the average of the five Q-band time traces.

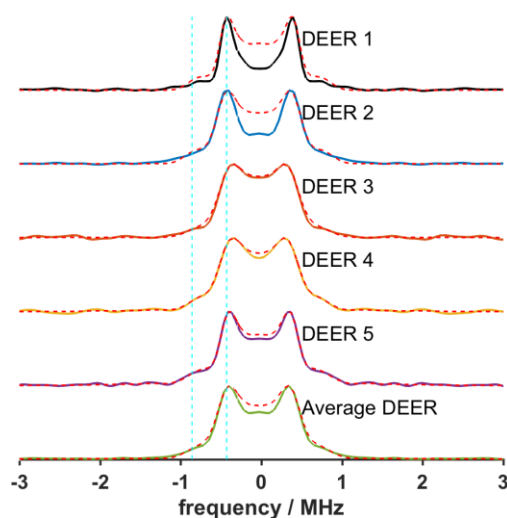


Figure S.14. Fast Fourier Transforms of the Q-band time traces (background corrected) in Figure S.13 given by DeerAnalysis2016⁷ demonstrating only small changes in the Pake pattern upon experiment variation. The dotted red lines show the distance distributions fits in the frequency domain. The cyan lines are at the singularity of the Pake pattern and the double frequency which fits to the high frequency shoulder and thus demonstrates that the exchange coupling is negligible.

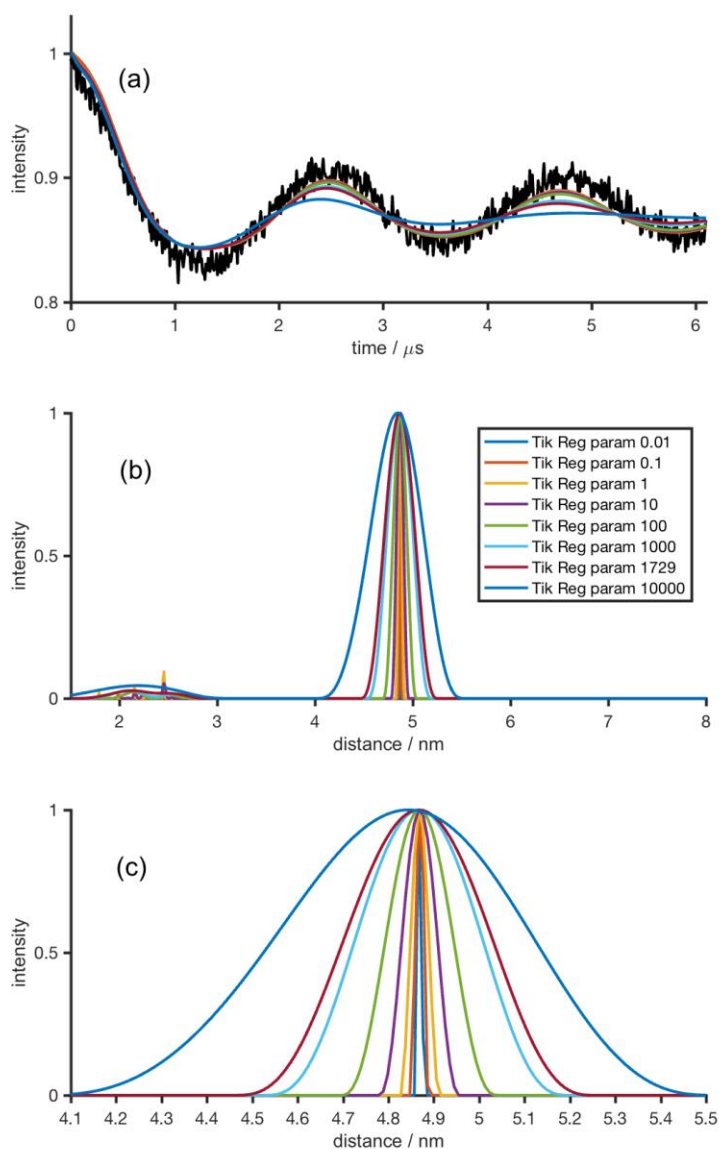


Figure S.15. Justification for using a Tikhonov Regularisation parameter of 10 for obtaining the distance distribution from DeerAnalysis2016⁷ shown in the main paper: a) background corrected DEER 1 data with fits from various regularisation parameters shown with coloured lines, key shown in figure (b). The value of 1729 was the number suggested by DeerAnalysis2016 but it can be seen to be not fitting the later modulations in the data and therefore will lead to a broadened distance distribution; b) resulting distance distributions for the various Tikhonov Regularisation parameters over the full range 1.5 to 8 nm; c) distance distributions as in (b) but in the range 4.1 to 5.5 nm to allow a comparison. A value of 10 was chosen for the main paper since this produced a good fit by eye to the DEER time trace, and gave an upper estimate for the distribution of the distances in (Y@C₈₂)₂•1 evident from the experiment.

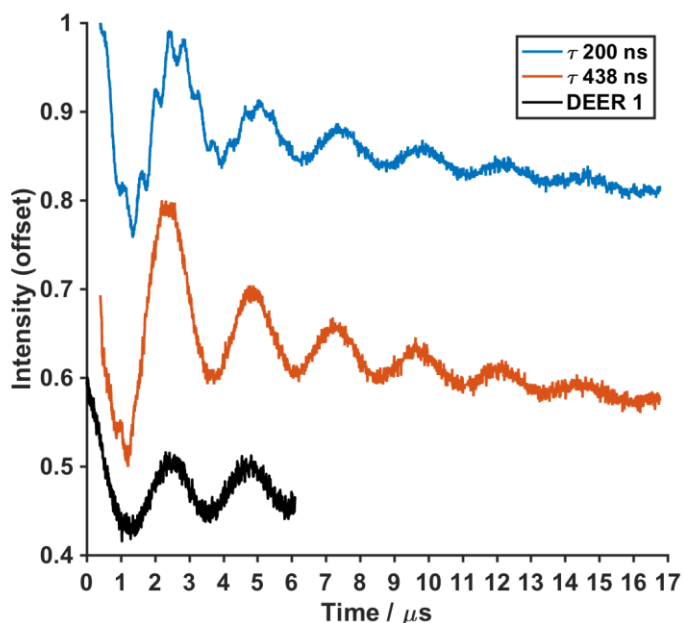


Figure S.16. Three-pulse electron spin echo envelope modulation (ESEEM) data performed at X-band compared to the background corrected Q-band DEER 1 (shown in the main paper) for $(Y@C_{82})_2\cdot 1$ in deuterated toluene. The ESEEM pulses were placed at the maximum of the field sweep spectrum with τ delay values given in the legend at 30 K and $\pi/2$ of 20 ns. This demonstrates the remarkable similarity between the ESEEM signal at X-band, due to coupling of the electron to the ^{89}Y nucleus, and the dipolar coupling frequency in the complex.

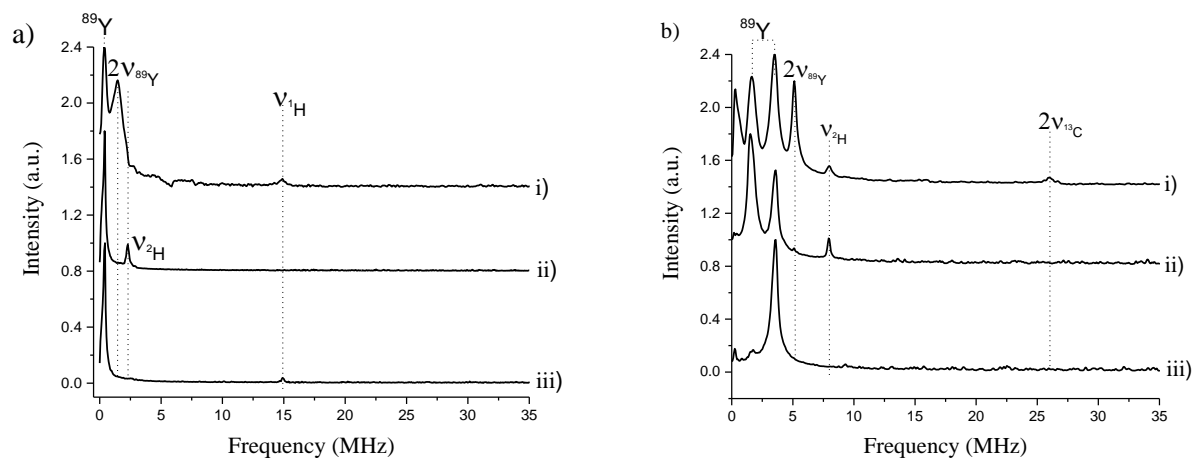


Figure S.17. Frequency domain spectra of two- and three-pulse ESEEM data performed at X- and Q-band for $(Y@C_{82})_2\cdot 1$ in deuterated toluene. The ESEEM pulses were placed at the maximum of the field sweep spectrum. The individual time domain trace was background corrected, apodized with a hamming window and zero-filled prior to Fourier Transformation. a) X-band ESEEM data, i) two-pulse ESEEM, ii) three-pulse ESEEM with $\tau = 200$ ns and iii) $\tau = 438$ ns. b) Q-band ESEEM data, i) two-pulse ESEEM, ii) three-pulse ESEEM with $\tau = 160$ ns and iii) $\tau = 250$ ns. Dotted lines correspond to the assignment of the peaks.

References:

- ¹ Terekhov, D. S.; Nolan, K. J.; McArthur, C. R.; Leznoff, C. C., *J. Org. Chem.* **1996**, 61, (9), 3034-3040.
- ² Higgins, R. W.; Hilton, C. L.; Willard, M. L.; Francis, H. J., *J. Org. Chem.* **1951**, 16, (10), 1577-1581.
- ³ Ishizaki, M.; Hoshino, O., *Tetrahedron* **2000**, 56, (45), 8813-8819.
- ⁴ Shinohara, H., *Rep. Prog. Phys.* **2000**, 63, 843-892.
- ⁵ Gil-Ramírez, G.; Karlen, S. D.; Shundo, A.; Porfyraakis, K.; Ito, Y.; Briggs, G. A. D.; Morton J. J. L.; and Anderson, H. L., *Org. Lett.*, **2010**, 12, 3544-3547.
- ⁶ HySS2009 is an updated version of the older version reported in: Alderighi, L.; Gans, P.; Ienco, A.; Peters, D.; Sabatini, A.; Vacca, A., *Coord. Chem. Rev.* **1999**, 184, 311-318.
- ⁷ Jeschke, G.; Chechik, V.; Ionita, P.; Godt, A.; Zimmermann, H.; Banham, J.; Timmel, C. R.; Hilger, D.; Jung, H., *Appl. Magn. Reson.*, **2006**, 30, 473-498.
- ⁸ Polyhach, Y.; Bordignon, E.; Tschaggelar, R.; Gandra, S.; Godt, A.; and Jeschke, G., *Phys. Chem. Chem. Phys.*, **2012**, 14, 10762-10773.